



Biological Role of Site-specific O-glycosylation in Cell Adhesion Activity and Phosphorylation of Osteopontin

メタデータ	言語: English 出版者: 公開日: 2019-06-27 キーワード (Ja): キーワード (En): 作成者: 大山, 翠 メールアドレス: 所属:
URL	https://fmu.repo.nii.ac.jp/records/2000251

学 位 論 文

**Biological Role of Site-specific *O*-glycosylation in
Cell Adhesion Activity and Phosphorylation of Osteopontin**

オステオポンチンの細胞接着活性とリン酸化における
部位特異的 *O*-結合型糖鎖修飾の生物学的役割

2018 年（平成 30 年）度

Midori Oyama

Department of Biochemistry,

Fukushima Medical University Graduate School of Medicine

福島県立医科大学大学院医学研究科医学専攻

生化学講座 分子調節学分野

大山 翠

論文内容要旨 (和文)

学位論文題名	Biological role of site-specific <i>O</i> -glycosylation in cell adhesion activity and phosphorylation of osteopontin オステオポンチンの細胞接着活性とリン酸化における部位特異的 <i>O</i> -結合型糖鎖修飾の生物学的役割
<p>オステオポンチン (osteopontin : OPN) は、細胞外に分泌されるリン酸化糖タンパク質である。OPN の発現は、多くの癌において悪性化に伴い上昇し、患者の予後不良と相関する。OPN は癌細胞の接着や運動、増殖を促進する。OPN のそうした活性の発現は、主に細胞表面受容体インテグリン $\alpha\text{v}\beta 3$ や $\alpha 5\beta 1$ を介しておこなわれるが、その相互作用には OPN リン酸化の関与が考えられている。</p> <p>糖鎖修飾は、ほとんどの膜および分泌タンパク質に付加される翻訳後修飾のひとつである。糖鎖はタンパク質の機能を調節し、様々な生体反応に関与する。しかしながら、タンパク質の糖鎖と機能に関する分子レベルでの解析はほとんどなされていないのが現状である。</p> <p>以前、私たちは、OPN 内のスレオニン/プロリンリッチ領域に存在する 5 か所の <i>O</i>-結合型糖鎖付加部位 (Thr¹³⁴/Thr¹³⁸/Thr¹⁴³/Thr¹⁴⁷/Thr¹⁵²) を欠損させたところ、OPN の細胞接着活性とリン酸化が上昇することを見出した。本研究では、OPN の糖鎖による活性調節機構をより詳細に検討するため、部位特異的 <i>O</i>-結合型糖鎖修飾をもつ組換え型 OPN の細胞接着活性およびリン酸化について調べた。</p> <p>そのために糖鎖を部位特異的に 1 か所あるいは複数か所欠損させた OPN を作製した。前側 2 か所 (Thr¹³⁴/Thr¹³⁸)、後側 3 か所 (Thr¹⁴³/Thr¹⁴⁷/Thr¹⁵²) の糖鎖付加部位を欠損した OPN は、野生型に比べ、それぞれ細胞接着活性の低下および上昇がみられた。一方、糖鎖付加部位を 1 か所のみ欠損した OPN は野生型と同程度の活性を示した。</p> <p>OPN と受容体との相互作用に対する糖鎖の影響を調べるため、インテグリン $\alpha\text{v}\beta 3$ と $\beta 1$ の機能阻害抗体やインテグリン $\alpha\text{v}\beta 3$ 高発現細胞を用いて、各組換え型 OPN に対する細胞接着アッセイをおこなった。その結果、OPN とそれらインテグリンとの相互作用に OPN 糖鎖が関与することが明らかとなった。</p> <p>質量分析やリン酸基を特異的に認識する Phos-tag を用いた ELISA 解析から、OPN のリン酸化レベルやリン酸化部位が糖鎖の付加状態に影響されることがわかった。また、OPN のリン酸化レベルと <i>O</i>-結合型糖鎖の数、細胞接着活性は必ずしも相関しないことが明らかとなった。</p> <p>これらの結果は、OPN の <i>O</i>-結合型糖鎖による細胞接着活性およびリン酸化の新たな調節機構を示唆するものである。</p>	

(Biochemical Journal, May 9, 2018, 475, 1583–1595)

Biological Role of Site-specific *O*-glycosylation in Cell Adhesion Activity and Phosphorylation of Osteopontin.

Midori Oyama*, Yoshinobu Kariya¹, Yukiko Kariya*, Kana Matsumoto[†], Mayumi Kanno*, Yoshiki Yamaguchi[†], Yasuhiro Hashimoto**¹**

*Department of Biochemistry, Fukushima Medical University School of Medicine, 1 Hikarigaoka, Fukushima City, Fukushima 960-1295, Japan; [†]Structural Glycobiology Team, Systems Glycobiology Research Group, RIKEN Global Research Cluster, 2-1 Hirosawa, Wako, Saitama 351-0198, Japan

¹To whom correspondence should be addressed: Department of Biochemistry, Fukushima Medical University School of Medicine, 1 Hikarigaoka, Fukushima City, Fukushima 960-1295, Japan. Tel: +81-24-547-1144; Fax: +81-24-548-8641; E-mail: kariya@fmu.ac.jp (Yoshinobu Kariya) or yasuc@fmu.ac.jp (Yasuhiro Hashimoto)

Short title: Site-specific *O*-glycosylation of Osteopontin

Keywords: osteopontin, *O*-glycosylation, cell adhesion, integrin, phosphorylation

The abbreviations used are: Arg–Gly–Asp, RGD; Arg–Gly–Glu, RGE; calf intestine alkaline phosphatase, CIAP; Coomassie Brilliant Blue, CBB; enzyme linked immunosorbent assay, ELISA; family with sequence similarity member 20C, Fam20C; horseradish peroxidase, HRP; low density lipoprotein, LDL; N-acetylgalactosamine, GalNAc; *O*-glycosylation site-defective, ΔO ; Osteopontin, OPN; recombinant OPN, rOPN; TBS containing 0.05% Tween-20, TBS-T; wild type, WT

ABSTRACT

Osteopontin (OPN) is an extracellular glycosylated phosphoprotein that promotes cell adhesion by interacting with several integrin receptors. We previously reported that an OPN mutant lacking five *O*-glycosylation sites (Thr¹³⁴/Thr¹³⁸/Thr¹⁴³/Thr¹⁴⁷/Thr¹⁵²) in the threonine/proline-rich region increased cell adhesion activity and phosphorylation compared with the wild type. However, the role of *O*-glycosylation in cell adhesion activity and phosphorylation of OPN remains to be clarified. Here, we show that site-specific *O*-glycosylation in the threonine/proline-rich region of OPN affects its cell adhesion activity and phosphorylation independently and/or synergistically. Using site-directed mutagenesis, we found that OPN mutants with substitution sets of Thr¹³⁴/Thr¹³⁸ or Thr¹⁴³/Thr¹⁴⁷/Thr¹⁵² had decreased and increased cell adhesion activity, respectively. In contrast, the introduction of a single mutation into the *O*-glycosylation sites had no effect on OPN cell adhesion activity. An adhesion assay using function-blocking antibodies against $\alpha\beta3$ and $\beta1$ integrins, as well as $\alpha\beta3$ integrin-overexpressing A549 cells, revealed that site-specific *O*-glycosylation affected the association of OPN with the two integrins. Phosphorylation analyses using phos-tag and LC-MS/MS indicated that phosphorylation levels and sites were influenced by the *O*-glycosylation status, although the number of *O*-glycosylation sites was not correlated with the phosphorylation level in OPN. Furthermore, a correlation analysis between phosphorylation level and cell adhesion activity in OPN mutants with the site-specific *O*-glycosylation showed that they were not always correlated. These results provide conclusive evidence of a novel regulatory mechanism of cell adhesion activity and phosphorylation of OPN by site-specific *O*-glycosylation.

Summary statement

Osteopontin is an extracellular glycosylated phosphoprotein that plays important roles in various physiological and pathological phenomena. The present study provides conclusive evidence of a novel regulatory mechanism of cell adhesion activity and phosphorylation of osteopontin by site-specific *O*-glycosylation.

INTRODUCTION

Osteopontin (OPN) is a secreted phosphoglycoprotein containing an Arg-Gly-Asp (RGD) sequence that binds to multiple integrins, such as $\alpha 5\beta 1$, $\alpha v\beta 1$, and $\alpha v\beta 3$ (1, 2), and also interacts with CD44 at its carboxyl-terminus (3). OPN interaction with these integrins as well as CD44 regulates several cellular functions, such as cell adhesion, migration, and proliferation through the activation of several cellular signaling pathways, such as ERK, NF- κ B, and Akt (4-7). OPN was originally identified as a transformation-specific phosphoprotein (8). Although increased OPN expression has been observed in various types of cancer cells and tumor tissues (9-11), it is also expressed by various types of normal cells and is found in most tissues and body fluids, such as blood, urine, bile, cerebrospinal fluid, and milk (12). In addition, OPN plays key roles in various physiological and pathological processes, including bone mineralization, wound healing, inflammation, autoimmune disease, and cancer metastasis (12-14).

Among extracellular proteins, OPN has one of the largest proportions of phosphorylation sites; to date, more than 36 potential phosphorylation sites have been identified (15-18). Furthermore, the extent of phosphorylation varies depending on the source of OPN. Recent studies have revealed that OPN is mainly phosphorylated by a secreted protein kinase, family with sequence similarity member 20C (Fam20C) (19, 20). Mutations in Fam20C cause Raine-syndrome, a severe osteosclerotic bone dysplasia that often results in death during the neonatal period, and the enzyme activity for phosphorylating OPN correlates to the disease severity (19, 21). Many studies have shown that the phosphorylation of OPN positively regulates interaction with cell surface receptors and its functional activities such as cell adhesion and migration. For example, partial dephosphorylation of OPN by osteoclastic tartrate-resistant acid phosphatase was shown to decrease its cell adhesion activity against osteoclasts (22). Furthermore, the phosphorylated form of OPN has been reported to preferentially interact with the cell surface rather than the non-phosphorylated form of OPN (23). In contrast, OPN phosphorylation also negatively regulates cellular functions. In one study, OPN phosphorylation by casein kinase II promoted its cell adhesion activity toward osteoclasts but not osteoblasts (24). Moreover, the adhesion of MDA-MB435 cells to human milk OPN was reported to be enhanced by dephosphorylation of OPN with alkaline phosphatase (25). These results indicate that the relationship between phosphorylation levels and functional activities of OPN needs to be carefully examined.

Mucin type *O*-glycosylation (hereafter referred to as *O*-glycosylation) is one of the most abundant forms of post-translational modification of secreted and membrane-bound proteins. *O*-glycosylation influences the conformation, secretion, and proteolytic processing of the attached proteins (26-30), thereby affecting cellular functions such as cell adhesion and migration (31, 32). Human OPN contains five *O*-glycosylation sites (Thr¹³⁴, Thr¹³⁸, Thr¹⁴³, Thr¹⁴⁷, and Thr¹⁵²) in the threonine/proline-rich region (Figure 1, WT), and these sites are well conserved among mammalian sequences (12). Our previous study revealed that an OPN mutant with deletion of all five *O*-glycosylation sites (ΔO) increased its cell adhesion activity compared with wild-type (WT) OPN (17). In addition, the study also showed that ΔO exhibited increased phosphorylation compared to the WT, and that dephosphorylation of ΔO increased cell adhesion activity (17). These results suggest that *O*-glycosylation of OPN directly, and possibly also indirectly through modulating the phosphorylation state, regulates its cell adhesion activity. However, it remains unknown whether there are *O*-glycosylation sites specifically for cell adhesion activity and phosphorylation of OPN. Site-specific *O*-glycosylation plays pivotal roles in protein function (33, 34). Given the significant role of *O*-glycosylation on OPN in cell adhesion activity and phosphorylation, it is important to determine their crucial sites. In the present study, using the recombinant OPNs (rOPNs) with site-specific *O*-glycosylation, we investigated the contribution of site-specific *O*-glycosylation to cell adhesion activity and phosphorylation of OPN.

EXPERIMENTAL

Expression vectors

His-tagged human OPN cDNA in pENTR_{TM}/D-TOPO[®] vector (Thermo Fisher Scientific; #K2400-20) was used to generate *O*-glycosylation site mutants by oligonucleotide site-directed mutagenesis (17). The final OPN constructs were recombined from pENTR_{TM}/D-TOPO[®] to a pcDNA6.2/V5-DEST Gateway vector (Thermo Fisher Scientific; #12489-027) using LR Clonase II Enzyme mix (Thermo Fisher Scientific; #11791). Human β 3 integrin cDNA was amplified by PCR using specific primer sets (Human ITGB3A-JJF: 5'-CGGGAGGCGGACGAGATGCGAGCGC-3' and Human ITGB3A-JJR: 5'-TTATCATTAAGTGCCCCGGTACGTGATATTGGTG-3') and KOD Plus polymerase (TOYOBO; #KOD-201) from the reverse-transcribed product of total RNA derived from the A549 human lung cancer cell line. The amplified product was treated with a 10 \times A-attachment mix (TOYOBO; #TAK-301) for the addition of 3' A-overhangs, and was then cloned into a pcDNA3.3-TOPO[®] vector (Invitrogen; #K8300-01) according to the manufacturer's instructions. The vector was then used as a template of PCR for the cloning of human β 3 integrin cDNA into the pENTR_{TM}/D-TOPO[®] vector. Next, the human β 3 integrin cDNA was recombined from pENTR_{TM}/D-TOPO[®] to a LZRS blast retroviral vector (a gift from Dr. M Peter Marinkovich) via the Gateway LR reaction. All cDNA sequences were verified by sequencing at each step.

Cell culture

Human embryonic kidney cells (HEK293T), modified human 293 phoenix cells (a gift from Dr. M Peter Marinkovich), human fibrosarcoma cells (HT1080), human breast cancer cells (MDA-MB231), and human lung cancer cells (A549) were cultured in Dulbecco's modified Eagle's medium (WAKO; #043-30085) supplemented with 10% FBS, and penicillin-streptomycin sulfate (WAKO; #168-23191).

Generation of HEK293T cells stably expressing His-tagged OPN

HEK293T cells that stably expressed His-tagged OPNs were generated as described previously (17). In brief, an expression vector was transfected into HEK293T cells using Lipofectamine[®] LTX and PLUS transfection reagents (Thermo Fisher Scientific; #A12621). The cells were selected in the presence of 10 μ g/ml blasticidin S (Merck Millipore; #203350).

Purification of recombinant OPN

His-tagged rOPN was purified from the serum-free conditioned medium of a HEK293T transfectant as described previously (17). The buffer of rOPN protein-containing fractions from Nickel Magnetic Beads (Merck Millipore; #LSKMAGH02) was exchanged with PBS including 0.1% CHAPS by ultrafiltration using Amicon Ultra Centrifugal Filters-30 kDa (Merck Millipore; # UFC503024). The concentrated protein was used for assays as a purified rOPN protein.

OPN dephosphorylation

In the dephosphorylation experiments, the samples were incubated with calf intestine alkaline phosphatase (CIAP, TOYOBO; #CAP-101) (1.5 units/ μ g OPN) at 37°C for 6 h, and subjected to the following assays.

SDS-PAGE, CBB staining and Western blot

Protein samples were separated on 7.5% (WAKO; #194-14931) or 5–20% (WAKO; #194-15021) SuperSept™ Ace gel under reducing conditions, and then stained with Coomassie Brilliant Blue (CBB). For Western blot analysis, proteins resolved by SDS/PAGE were transferred onto a nitrocellulose membrane. The membrane was blocked with 1% BSA in PBS for 1 h at room temperature and then incubated with a rabbit polyclonal antibody against human OPN (IBL, clone O-17; #18625). After incubation with horseradish peroxidase (HRP)-conjugated anti-rabbit IgG antibody (Promega; #W4018), the membranes were developed using the SuperSignal West Dura Extended Duration Substrate kit (Thermo Fisher Scientific; #34075).

Cell adhesion assay

Cell adhesion assays were performed as described previously (17). In brief, the wells of a 96-well plate (Costar; #3590) were coated with 50 μ l of an indicated concentration of rOPN proteins, and blocked with 1% BSA in PBS. Cell suspensions in serum-free medium were plated into each well (5×10^4 cells/well) and incubated at 37°C for 1 h in a 5% CO₂ incubator. After removing all non-adherent cells by vigorous shaking, the remaining adherent cells were fixed with 25% (w/v) glutaraldehyde for 10 min and stained with 0.5% crystal violet in 20% (v/v) methanol for 10 min. After extracting the dye using 0.1 M sodium citrate in 50% methanol (v/v) for 30 min, the absorbance at 590 nm was measured using a microplate reader (BioRad; model 680). For inhibition assays, cell suspensions were incubated with PBS, EDTA, control

Gly–Arg–Gly–Glu–Ser–Pro (GRGESp) and Gly–Arg–Gly–Asp–Ser–Pro (GRGDSP) peptides (Takara; #SP002 and SP001), mouse IgG (Santa Cruz Biotechnology; #sc-2025), or function-blocking antibodies against $\alpha\beta3$ (Merck Millipore, clone LM609; # MAB1976) and $\beta1$ integrins (Merck Millipore, clone JB1A; #MAB1965), and CD44 (Thermo Fisher Scientific, Hermes-1; #MA4400) at room temperature for 20 min before inoculation.

Enzyme-linked immunosorbent assay

The 96 wells of an enzyme linked immunosorbent assay (ELISA) plate (Thermo Fisher Scientific; #445101) were coated with 50 μ l of rOPN proteins overnight at 4°C, blocked with 1% BSA in PBS for 1 h at 37°C, washed three times with TBS containing 0.05% Tween-20 (TBS-T), and then incubated with 0.01 μ g/ml anti-OPN monoclonal antibody (IBL, clone 10A16; #10011) for 1 h at 37°C. The wells were then washed three times with TBS-T, followed by incubation for 1 h at 37°C with HRP-conjugated goat anti-mouse IgG antibody (1:5000, Cell Signaling; #7076). To detect the phosphorylated forms of rOPN, the wells of the ELISA plate coated with rOPNs were washed three times with TBS-T and incubated with HRP-conjugated phos-tag solution (WAKO; #301-93531) for 3 h at room temperature. After washing the wells three times with TBS-T, color development was obtained using the TMB microwell peroxidase substrate system (KPL; #50-76-11), and the reaction was stopped by phosphoric acid. The color intensity was measured at 450 nm using a microplate reader (BioRad; model 680).

LC-MS/MS analysis

Purified rOPNs (34 pmol each) were dissolved in 200 μ l of 50 mM NH_4HCO_3 with 2% (v/v) acetonitrile and 0.1% (v/v) trifluoroacetic acid. A mixture of trypsin and lysyl endopeptidase or endoproteinase Asp-N was added to a sample with a substrate/enzyme ratio of 50 (w/w) and incubated at 37°C for 16 h. The resulting peptides were analyzed with an EASY-nLC 1000 HPLC system (Thermo Fisher Scientific) coupled to a Q Exactive mass spectrometer (Thermo Fisher Scientific). The peptides were separated with a NANO-HPLC capillary column (C18, 0.075 \times 150 mm; Nikkyo Technos) using an acetonitrile gradient in 0.1% (v/v) formic acid at a flow rate of 0.3 μ l/min: 5–35% (v/v) for 0–48 min, and 35–65% (v/v) for 48–60 min. MS and MS/MS analyses were performed in the positive ion mode and the acquired data were analyzed using the Proteome Discover software (ver. 1.4; Thermo Fisher Scientific) with the MASCOT search engine (ver. 2.5.1; Matrix Science, London, UK). SwissProt 2013_03 (Homo sapiens, 20,329 sequences) was used for MS data matching. The site probabilities of phosphorylation

were calculated using the phosphoRS tool. In order to avoid ambiguity with regard to the phosphorylation sites, only those with more than 99% probability are shown in the data, and are discussed in the text. To identify the *O*-glycosylation sites in the threonine/proline-rich region, purified rOPNs were treated with CIAP/sialidase or CIAP. Then the samples were digested with trypsin/lysyl endopeptidase, endoproteinase Asp-N, V8 protease or a mixture of them and the resulting peptides were subjected to the LC-MS/MS analysis.

Generation of A549 cells stably overexpressing $\beta 3$ integrin

Retrovirus infection was performed as described previously (35). In brief, human $\beta 3$ integrin and control lacZ in LZRS blast retroviral vectors were independently transfected into 293 phoenix cells using FuGENE®6 transfection reagent, then cells were selected with 5 μ g/ml puromycin. A549 cells were infected with the retrovirus that was produced in the 293 phoenix cells, and were then selected with 10 μ g/ml blasticidin S.

Flow cytometry analysis

Cells were detached from a 10-cm dish using trypsin with 1 mM EDTA. After quenching trypsinization with a medium that contained 10% FBS, the cells were washed twice with PBS containing 1 mM EDTA, and then incubated with an anti- α v $\beta 3$ integrin antibody (Biolegend, clone 23C6; #304402) or control IgG on ice for 30 min. The cells were washed three times with PBS containing 1 mM EDTA, followed by incubation for 15 min with Alexa Fluor 488-conjugated goat anti-mouse IgG antibody (Thermo Fisher Scientific; #A11029). Finally, the cells were analyzed by flow cytometry using FACSCalibur and CellQuest software (BD Biosciences).

Statistical analysis

The results are given as mean \pm standard error and are representative of at least two or three independent experiments, each conducted in triplicate. Statistical comparisons were made among the groups using one-way ANOVA followed by a Bonferroni post-test. A P value of < 0.05 was considered significant. Spearman's rank correlation analysis was used for the statistical analysis of correlations between phosphorylation level and cell adhesion activity. All statistical analyses were performed with GraphPad Prism Version 6.0 software.

RESULTS

Establishment of various O-glycosylation site-defective OPN mutants overexpressing HEK293T cells

Human OPN has five *O*-glycosylation sites in the threonine/proline-rich region, Thr¹³⁴, Thr¹³⁸, Thr¹⁴³, Thr¹⁴⁷, and Thr¹⁵² (Figure 1, WT). We previously found that an OPN mutant with all five *O*-glycosylation sites defective (Figure 1, ΔO) increased both cell adhesion activity and phosphorylation level compared with the WT (17). These results suggest that *O*-glycosylation affects both cell adhesion activity and phosphorylation in OPN, and that OPNs with a different *O*-glycosylation status might have distinct cell adhesion activity and phosphorylation status. To investigate this possibility, we prepared single or multiple *O*-glycosylation site-defective OPN mutants by replacing the threonine residue in the *O*-glycosylation site of the threonine/proline-rich region with alanine residues (shown in Figure 1) as follows: five variants with a single mutation, $\Delta 1$ – $\Delta 5$ (T134A, T138A, T143A, T147A, and T152A), one variant with a double mutation, $\Delta 1/2$ (T134A/T138A), and one variant with a triple mutation, $\Delta 3/4/5$ (T143A/T147A/T152A). The cDNA expression vectors were independently transfected into HEK293T cells, and then the cell lines stably expressing OPN mutants were established after selection with blasticidin S.

Characterization of purified rOPN mutants

To purify the rOPNs, the conditioned medium of the HEK293T transfectant was applied to nickel affinity chromatography and heparin sepharose chromatography. The purified rOPN proteins were analyzed by SDS-PAGE under reducing conditions. CBB staining revealed that each rOPN consisted of two bands, which were predicted to be non-cross-linked OPN (Figure 2A, upper band) and intramolecularly cross-linked OPN which was catalyzed by transglutaminase 2 (Figure 2A, lower band) (36). Western blot with an anti-OPN polyclonal antibody (O-17; Figure 2B) identified 62 and 57 kDa bands in the WT, 57 and 53 kDa bands in ΔO , 61 and 57 kDa bands in $\Delta 1$ – $\Delta 5$, 60 and 56 kDa bands in $\Delta 1/2$, and 59 and 55 kDa bands in $\Delta 3/4/5$ as OPN proteins (Figure 2A and 2B). The ΔO , $\Delta 1$ – $\Delta 5$, $\Delta 1/2$, and $\Delta 3/4/5$ bands migrated faster than the WT bands in an SDS-PAGE gel, which we assumed was mainly due to a lack of *O*-glycosylation (Figure 2A and 2B).

Cell adhesion activity of O-glycosylation site-defective OPN mutants

To clarify the relationship between the site-specific *O*-glycosylation and the functional activity of OPN, we tried to study the cell adhesion activity of the purified rOPN mutants. First, we investigated the cell adhesion activity of multiple *O*-glycosylation site-defective OPN, $\Delta 1/2$, $\Delta 3/4/5$, and ΔO as well as WT using human fibrosarcoma HT1080 cells (Figure 3A). As previously described (17), the cell adhesion activity of ΔO was higher than that of the WT (Figure 3A, WT vs ΔO). $\Delta 3/4/5$ showed the strongest cell adhesion activity in the test samples (Figure 3A, $\Delta 3/4/5$ vs ΔO , WT, and $\Delta 1/2$). Conversely, $\Delta 1/2$ indicated the weakest cell adhesion activity in the test samples (Figure 3A, $\Delta 1/2$ vs WT, ΔO , and $\Delta 3/4/5$). We also investigated the cell adhesion activity using the same samples against human breast cancer MDA-MB231 cells. A similar result to Figure 3A was also obtained in this condition; that is, ΔO indicated about 1.3-fold higher cell adhesion activity than the WT, and $\Delta 3/4/5$ and $\Delta 1/2$ exhibited the highest and lowest cell adhesion activity in the tested samples, respectively (Figure 3B).

To further determine whether a specific *O*-glycosylation site for the cell adhesion activity of OPN was present or not, the cell adhesion activity of single *O*-glycosylation site-defective OPN mutants ($\Delta 1$, $\Delta 2$, $\Delta 3$, $\Delta 4$, and $\Delta 5$) was also examined using MDA-MB231 cells. These single site-defective mutants showed almost the same cell adhesion activity as the WT (Figure 3C).

To explore the possibility of differential plate-coating efficiency of rOPNs, we used an ELISA method using an anti-OPN antibody, 10A16, epitope of which does not contain phosphorylation sites or glycosylation sites in rOPNs. There was no difference in the coating efficiency among all tested rOPNs (Figure 3D). We also tested the plate-coating efficiency of rOPNs using another anti-OPN antibody, O-17, which recognizes N-terminal amino acid sequences in OPN that contains no phosphorylation sites or glycosylation sites. The result was similar to that of ELISA using 10A16 (data not shown), indicating that the difference in the adhesive activities of rOPNs was not likely due to differential binding of the proteins to the plastic plates. These results indicate that the deletion of multiple *O*-glycosylation sites rather than a single *O*-glycosylation site may influence the cell adhesion activity of OPN.

Association of O-glycosylation site-defective OPN mutants with $\alpha v\beta 3$ integrin

OPN regulates its biological functions mainly through its association with integrins; thus, we hypothesized that multiple *O*-glycosylation site-defective OPN, ΔO , $\Delta 1/2$, and $\Delta 3/4/5$ changed

their cell adhesion activity as a consequence of altered integrin associations, especially $\alpha\beta3$ integrin, which is a primary receptor for OPN. We then examined the inhibitory effects of EDTA, RGD peptide, and a function-blocking antibody against $\alpha\beta3$ integrin on the cell adhesion activity of the WT, ΔO , $\Delta 1/2$, and $\Delta 3/4/5$ (Figure 4A and 4B). EDTA and RGD peptide completely blocked cell adhesion in all tested samples (Figure 4B). A function-blocking antibody against $\alpha\beta3$ integrin efficiently blocked cell adhesion to the WT ($93 \pm 0.90\%$ inhibition), and $\Delta 1/2$ ($85 \pm 5.7\%$ inhibition). In contrast, ΔO ($31 \pm 9.1\%$ inhibition) and $\Delta 3/4/5$ ($17 \pm 7.6\%$ inhibition) were resistant to the inhibitory effect of the antibody (Figure 4B).

To better understand the interaction of each rOPN with $\alpha\beta3$ integrin, we examined the cell adhesion activity of each rOPN using A549 cells overexpressing $\beta3$ integrin (Figure 4A, $\beta3$ -A549), which highly expressed $\alpha\beta3$ integrin (Figure 4C). Also we prepared lacZ-A549 cells, which expressed little $\alpha\beta3$ integrin and were used as a control. When lacZ-A549 cells were plated on the rOPNs, the cells could efficiently adhere to ΔO and $\Delta 3/4/5$ compared with WT and $\Delta 1/2$ (Figure 4D, lacZ-A549). The cell adhesion activities of WT and $\Delta 1/2$ were increased by $\alpha\beta3$ integrin overexpression to a similar extent to ΔO and $\Delta 3/4/5$ (Figure 4D, $\beta3$ -A549), suggesting that, compared to ΔO and $\Delta 3/4/5$, the adhesion of WT and $\Delta 1/2$ to cells was largely dependent on the interaction with $\alpha\beta3$ integrin. We also examined the inhibitory effect of a function-blocking antibody against $\beta1$ integrin on cell adhesion to the rOPNs. The inhibitory effect of the $\beta1$ integrin antibody on cell adhesion to rOPNs, which we found to be similar to that of the anti- $\alpha\beta3$ integrin antibody (Figure 4B). These results indicate that site-specific *O*-glycosylation in OPN may influence the association with $\alpha\beta3$ and $\beta1$ integrins, thereby affecting the cell adhesion activity.

Furthermore, we examined the inhibitory effect of a function-blocking antibody against another receptor for OPN, CD44 on cell adhesion to the rOPNs. The neutralizing monoclonal antibody against CD44 had no effect on the cell adhesion of MDA-MB231 cells, which express CD44 on the cell surface, to all rOPNs (data not shown). These results suggest that the cell adhesion activity of these rOPNs was mediated mainly through RGD-dependent integrins but not CD44.

Phosphorylation status of O-glycosylation site-defective OPN mutants

Our previous study showed that the phosphorylation level increased in ΔO compared to the WT (17). To examine whether differentially *O*-glycosylated OPN has a distinct phosphorylation

status, we investigated the phosphorylation status of rOPN mutants by quantitative ELISA using a phos-tag that directly reacts with phosphorylated proteins (Figure 5A). Similar to our previous study (17), the phosphorylation level of the WT was quite low, whereas ΔO was phosphorylated almost 4-fold compared with the WT. The other mutants were phosphorylated to varying degrees; $\Delta 1$, $\Delta 3$, $\Delta 4$, and $\Delta 3/4/5$ showed similar phosphorylation levels to ΔO . Although the phosphorylation level of $\Delta 2$ was higher than that of the WT, it was the lowest level of the *O*-glycosylation mutants. In contrast, $\Delta 5$ and $\Delta 1/2$ showed higher reactivity with the phos-tag than ΔO . After phosphatase treatment, the phosphorylation levels in all *O*-glycosylation mutants were decreased to those of the WT, indicating that the quantitative ELISA using a phos-tag represented phosphorylated forms of rOPNs (Figure S1).

To better understand the relationship between *O*-glycosylation and phosphorylation, we also tried to identify the potential phosphorylation sites in rOPNs, $\Delta 1/2$ and $\Delta 3/4/5$ (Figure 5B, and Supplementary Tables S1–S4). The mixture of trypsin and lysyl endopeptidase- or Asp-N-digested peptides derived from $\Delta 1/2$ and $\Delta 3/4/5$ were analyzed by LC-MS/MS (Supplementary Tables S1–S4). The coverages of the identical peptides for each experiment were 66% (mixture of trypsin and lysyl endopeptidase) and 67% (Asp-N) for $\Delta 1/2$, and 69% (mixture of trypsin and lysyl endopeptidase) and 69% (Asp-N) for $\Delta 3/4/5$. The data obtained with the enzyme digestions were complementary and covered most of the OPN sequence. Finally, 18 and 16 phosphorylation sites were identified in the sequences of $\Delta 1/2$ and $\Delta 3/4/5$, respectively (Figure 5B). Twelve phosphorylated residues were common between $\Delta 1/2$ and $\Delta 3/4/5$, and phosphorylation at Ser¹²⁶, Ser¹²⁹, Tyr²²⁵, Ser²⁶⁷, Ser²⁸⁰, and Ser³⁰³, and at Ser⁸¹, Ser²²⁸, Ser²⁵⁸, and Ser²⁹¹ were the specific sites of $\Delta 1/2$ and $\Delta 3/4/5$, respectively (Figure 5B). We also confirmed that Thr¹⁴³, Thr¹⁴⁷, and Thr¹⁵² in $\Delta 1/2$, and Thr¹³⁴, and Thr¹³⁸ in $\Delta 3/4/5$ were *O*-glycosylated in the threonine/proline-rich region by LC-MS/MS analyses (Supplementary Table S5). Taken together, our findings indicated that the phosphorylation level and site were influenced by the *O*-glycosylation status in the threonine/proline-rich region.

Relationship between phosphorylation level and cell adhesion activity in OPN

Although many studies have reported that the phosphorylation of OPN is important for cell adhesion activity, there are also contradictory findings between the two (22–25). A correlation analysis between them revealed that no significant correlation was found between the phosphorylation level and cell adhesion activity in OPN (Figure 5C). We also found that

dephosphorylated ΔO and $\Delta 1/2$ increased MDA-MB231 cell adhesion activity after phosphatase treatment compared with phosphorylated ΔO and $\Delta 1/2$; however, WT and $\Delta 3/4/5$ with the same treatment had no effect (17) (Figure 5D). These results suggest that it is difficult to predict the cell adhesion activity of OPN only from its total phosphorylation level.

DISCUSSION

Our previous study indicated that *O*-glycosylation of OPN affects its cell adhesion activity and phosphorylation (17), but the extent to which the specific site of *O*-glycosylation has an effect remains unclear. Here, through analysis using rOPN proteins that sequentially lacked one or multiple *O*-glycosylation sites, we demonstrated that site-specific *O*-glycosylation in the threonine/proline-rich region of OPN affects its cell adhesion activity and phosphorylation independently or synergistically. Furthermore, comparative analysis between the cell adhesion activity and the phosphorylation level suggests that the degree of phosphorylation does not always correlate with cell adhesion activity in OPN.

In the present study, we purified rOPNs from the conditioned medium of HEK293T transfectants, and the two bands were detected in the immunoblots and CBB stainings (Figure 2). Considering the molecular sizes of two bands, this might be attributed to the transglutaminase 2-mediated cross-linking. Transglutaminase 2 cross-links OPN inter- or intramolecularly, which depend on the ratio of transglutaminase 2 to OPN (36). Although it has been reported that intermolecular cross-linking of OPN affected OPN functions such as cell adhesion and migration, the effect of intramolecular cross-linking of OPN on them remains unclear. Interestingly, Segers-Nolten et al. have shown that intramolecular cross-linking of Parkinson's disease-associated protein, α -synuclein catalyzed by tissue transglutaminase modulated its oligomerization. The tissue transglutaminase-mediated α -synuclein oligomers appear to be unstructured and are unstable to disrupt phospholipid vesicles compared to normal β -sheet-containing oligomers (37), suggesting that the OPN functions could be influenced by intramolecular cross-linking.

We also found significant changes in cell adhesion activity in multiple *O*-glycosylation site-defective OPN mutants, $\Delta 1/2$ and $\Delta 3/4/5$, as well as ΔO compared to the WT (Figure 3A and 3B). However, the deletion of a single *O*-glycosylation site had no effect on OPN cell adhesion activity (Figure 3C). These results support the idea that multiple *O*-glycosylation deficiencies in the threonine/proline-rich region affect the biological functions of OPN. This idea may be supported by Minai-Therani et al., who reported that lung cancer cells overexpressing an OPN mutant that lacked three *O*-glycosylation sites (Thr¹³⁸, Thr¹⁴⁷, and Thr¹⁵²) decreased cell growth and migration in vitro and in vivo (38). Our present study also demonstrated that the deletion of *O*-glycosylation sites, Thr¹⁴³, Thr¹⁴⁷, and Thr¹⁵², acquired

resistance to a function-blocking antibody against the $\alpha v\beta 3$ and $\beta 1$ integrins (Figure 4B, $\Delta 3/4/5$ and ΔO). Since the three *O*-glycosylation sites are proximal to the RGD sequence, which is a binding site for the $\alpha v\beta 3$, $\alpha 5\beta 1$, and $\alpha v\beta 1$ integrins (Figure 1), they may affect the association of OPN with the $\alpha v\beta 3$ and $\beta 1$ integrins. Moreover, the altered activities of rOPNs by deletion of *O*-glycosylation sites might be due to the conformational change of them. OPN contains a large number of acidic amino acids such as aspartic acids, phosphate groups, and sialic acids. Thus, the structure of OPN might be partly determined by their negative charges. In the OPN mutants, the deletion of *O*-glycans causes the decrease of negative charges because of loss of sialic acids on the depleted *O*-glycans. Therefore, the decreased negative charges might induce the conformational change of OPN, thereby affecting the interaction between rOPNs and integrins.

The isoforms of polypeptide *N*-acetylgalactosamine (GalNAc)-transferase are differentially expressed in cells and tissues during development and differentiation as well as various diseases including cancer (39). Because the *O*-glycosylation is mainly attributed to the expression pattern of polypeptide GalNAc-transferases, different site-specific *O*-glycosylation in the same core protein can occur. In the breast cancer cell line T47D, for example, the DTR motif within the MUC1 tandem repeats was nearly fully *O*-glycosylated at each of the five potential sites (40). In contrast, while all of these sites can be glycosylated, the average degree of *O*-glycosylation within the DTR motif for MUC1 from milk was only 50% (41). Such differences in the site-specific *O*-glycosylation pattern could generate distinct protein activities. The low density lipoprotein (LDL) receptor produced by a monensin-resistant CHO mutant cells lacks *O*-glycosylation at the selected first and/or second domain (42). The *O*-glycosylation-truncated LDL receptor exhibited greatly reduced binding to the ligand, LDL, than that expressed in normal CHO cells (43). Also, the *O*-glycosylation of calcitonin affected both the conformation and biological activity in a site-dependent manner (44). The expression of OPN functions largely depends on the interaction with integrins. Therefore, alteration in the association of OPN with integrins by changing the *O*-glycosylation state may be one of the regulatory mechanisms for OPN functions. If an OPN with various *O*-glycosylation patterns, including the mutants used in the current study, are present in vivo, *O*-glycan may regulate the biological functions of OPN in various physiological and pathological phenomena.

OPN carries a heterogeneous mixture of *O*-glycans, such as T-antigens, sialyl-Tn antigens, sialyl-T antigens, and other more elongated *O*-glycans (17,18,31). Although the *O*-glycan

structures in the five *O*-glycosylation sites in the threonine/proline-rich region were not determined in this study, the identification of *O*-glycan structures in the region may also be important for understanding the regulatory mechanisms of OPN functions by *O*-glycosylation. For example, sialic acid containing *O*-glycan may regulate such OPN-integrin interactions due to its negative charge because desialylation of OPN leads to the loss of cell surface binding ability (45). Site-directed mutagenesis by replacing threonine residues with alanine residues, as used in the present study, may eliminate the possibility of glycosylation at specific sites and also affect the degree of glycosylation at the remaining sites in an unknown manner (46). Further studies are required to elucidate the exact role of *O*-glycosylation in the function and modification of OPN.

Our present study showed that the degree of phosphorylation did not always correlate with cell adhesion activity in OPN, suggesting that it is difficult to predict the cell adhesion activity of OPN from its total phosphorylation level only. Although other modifications also affect the activity, it is possible that some site-specific phosphorylations, which may be induced by alteration of the *O*-glycosylation pattern, are one of the determinants of functional activities. In that case, the output of the biological functions induced by phosphorylation may be the result of the total effect of each specific phosphorylation-induced function in OPN. Further studies on the effect of phosphorylation at specific sites on the activities are required.

Phosphorylation of FGF23 on Ser¹⁸⁰ by Fam20C inhibits site-specific *O*-glycosylation on Thr¹⁷⁸ by GalNAc-T3 (47). In this case, phosphorylation of FGF23 might occur before *O*-glycosylation. The current study showed that phosphorylation of OPN was affected by *O*-glycosylation, suggesting that some OPN may be phosphorylated after *O*-glycosylation. Moreover, LC-MS/MS analysis revealed that Ser²⁵⁴ in $\Delta 1/2$, and Ser²¹⁹ and Ser²²⁸ in $\Delta 3/4/5$ were modified by both phosphorylation and *O*-glycosylation. These results suggest that the modification of OPN could be competitively regulated by phosphorylation and *O*-glycosylation. Therefore, phosphorylation of OPN may be controlled by *O*-glycosylation and vice versa. Considering the implications of OPN in various pathological processes, such as inflammation, autoimmune disease, and cancer metastasis (12–14), in which glycosylation and phosphorylation are dynamically regulated (15, 48), the understanding of the molecular mechanisms of OPN glycosylation and phosphorylation would be important for medical therapy in various OPN-related diseases and provide a clue to develop novel therapeutics.

ACKNOWLEDGEMENTS

The author thanks professor Ikuo Wada (department of cell science, institute of biomedical sciences), associate professor Masayuki Sekimata (department of biomolecular sciences, institute of biomedical sciences) and assistant professor Tomohito Higashi (department of basic pathology) for reviewing this study and valuable comments. I am grateful to Dr. M. Peter Marinkovich (Stanford University) for providing the vector and cells. I thank the Research Resources Center in Brain Science Institute (RIKEN) for the mass analysis and discussions. Finally, I sincerely thank professor Yasuhiro Hashimoto, associate professor Yoshinobu Kariya and members of the department of biochemistry for valuable scientific discussions and guiding my work with detailed comments.

DECLARATIONS OF INTEREST

The authors declare no competing financial interests.

FUNDING

This work was partially supported by a grant funding [grant number SO23016] from the Japan Intractable Diseases Research Foundation (Yoshinobu Kariya).

REFERENCES

1. Ross, F. P., Chappel, J., Alvarez, J. I., Sander, D., Butler, W. T., Farach-Carson, M. C., Mintz, K. A., Robey, P. G., Teitelbaum, S. L., and Cheresch, D. A. (1993) Interactions between the bone matrix proteins osteopontin and bone sialoprotein and the osteoclast integrin alpha v beta 3 potentiate bone resorption, *The Journal of biological chemistry* 268, 9901-9907.
2. Hu, D. D., Lin, E. C., Kovach, N. L., Hoyer, J. R., and Smith, J. W. (1995) A biochemical characterization of the binding of osteopontin to integrins alpha v beta 1 and alpha v beta 5, *The Journal of biological chemistry* 270, 26232-26238.
3. Rodrigues, L. R., Teixeira, J. A., Schmitt, F. L., Paulsson, M., and Lindmark-Mansson, H. (2007) The role of osteopontin in tumor progression and metastasis in breast cancer, *Cancer Epidemiol Biomarkers Prev* 16, 1087-1097.
4. Das, R., Mahabeleshwar, G. H., and Kundu, G. C. (2003) Osteopontin stimulates cell motility and nuclear factor kappaB-mediated secretion of urokinase type plasminogen activator through phosphatidylinositol 3-kinase/Akt signaling pathways in breast cancer cells, *The Journal of biological chemistry* 278, 28593-28606.
5. Das, R., Mahabeleshwar, G. H., and Kundu, G. C. (2004) Osteopontin induces AP-1-mediated secretion of urokinase-type plasminogen activator through c-Src-dependent epidermal growth factor receptor transactivation in breast cancer cells, *The Journal of biological chemistry* 279, 11051-11064.
6. Lin, Y. H., and Yang-Yen, H. F. (2001) The osteopontin-CD44 survival signal involves activation of the phosphatidylinositol 3-kinase/Akt signaling pathway, *The Journal of biological chemistry* 276, 46024-46030.
7. Scatena, M., Almeida, M., Chaisson, M. L., Fausto, N., Nicosia, R. F., and Giachelli, C. M. (1998) NF-kappaB mediates alphavbeta3 integrin-induced endothelial cell survival, *The Journal of cell biology* 141, 1083-1093.
8. Senger, D. R., Wirth, D. F., and Hynes, R. O. (1979) Transformed mammalian cells secrete specific proteins and phosphoproteins, *Cell* 16, 885-893.
9. Brown, L. F., Papadopoulos-Sergiou, A., Berse, B., Manseau, E. J., Tognazzi, K., Perruzzi, C. A., Dvorak, H. F., and Senger, D. R. (1994) Osteopontin expression and distribution in human carcinomas, *The American journal of pathology* 145, 610-623.
10. Coppola, D., Szabo, M., Boulware, D., Muraca, P., Alsarraj, M., Chambers, A. F., and Yeatman, T. J. (2004) Correlation of osteopontin protein expression and pathological

- stage across a wide variety of tumor histologies, *Clinical cancer research : an official journal of the American Association for Cancer Research* 10, 184-190.
11. Shevde, L. A., and Samant, R. S. (2014) Role of osteopontin in the pathophysiology of cancer, *Matrix biology : journal of the International Society for Matrix Biology* 37, 131-141.
 12. Sodek, J., Ganss, B., and McKee, M. D. (2000) Osteopontin, *Crit Rev Oral Biol Med* 11, 279-303.
 13. Kazanecki, C. C., Uzwiak, D. J., and Denhardt, D. T. (2007) Control of osteopontin signaling and function by post-translational phosphorylation and protein folding, *Journal of cellular biochemistry* 102, 912-924.
 14. Kariya, Y., Kariya, Y., Saito, T., Nishiyama, S., Honda, T., Tanaka, K., Yoshida, M., Fujihara, K., and Hashimoto, Y. (2015) Increased cerebrospinal fluid osteopontin levels and its involvement in macrophage infiltration in neuromyelitis optica, *BBA clinical* 3, 126-134.
 15. Yalak, G., and Vogel, V. (2012) Extracellular phosphorylation and phosphorylated proteins: not just curiosities but physiologically important, *Science signaling* 5, re7.
 16. Christensen, B., Nielsen, M. S., Haselmann, K. F., Petersen, T. E., and Sorensen, E. S. (2005) Post-translationally modified residues of native human osteopontin are located in clusters: identification of 36 phosphorylation and five O-glycosylation sites and their biological implications, *The Biochemical journal* 390, 285-292.
 17. Kariya, Y., Kanno, M., Matsumoto-Morita, K., Konno, M., Yamaguchi, Y., and Hashimoto, Y. (2014) Osteopontin O-glycosylation contributes to its phosphorylation and cell-adhesion properties, *The Biochemical journal* 463, 93-102.
 18. Li, H., Shen, H., Yan, G., Zhang, Y., Liu, M., Fang, P., Yu, H., and Yang, P. (2015) Site-specific structural characterization of O-glycosylation and identification of phosphorylation sites of recombinant osteopontin, *Biochimica et biophysica acta* 1854, 581-591.
 19. Tagliabracci, V. S., Engel, J. L., Wen, J., Wiley, S. E., Worby, C. A., Kinch, L. N., Xiao, J., Grishin, N. V., and Dixon, J. E. (2012) Secreted kinase phosphorylates extracellular proteins that regulate biomineralization, *Science (New York, N.Y.)* 336, 1150-1153.
 20. Ishikawa, H. O., Xu, A., Ogura, E., Manning, G., and Irvine, K. D. (2012) The Raine syndrome protein FAM20C is a Golgi kinase that phosphorylates bio-mineralization

- proteins, *PloS one* 7, e42988.
21. Simpson, M. A., Hsu, R., Keir, L. S., Hao, J., Sivapalan, G., Ernst, L. M., Zackai, E. H., Al-Gazali, L. I., Hulskamp, G., Kingston, H. M., Prescott, T. E., Ion, A., Patton, M. A., Murday, V., George, A., and Crosby, A. H. (2007) Mutations in FAM20C are associated with lethal osteosclerotic bone dysplasia (Raine syndrome), highlighting a crucial molecule in bone development, *Am J Hum Genet* 81, 906-912.
 22. Ek-Rylander, B., Flores, M., Wendel, M., Heinegard, D., and Andersson, G. (1994) Dephosphorylation of osteopontin and bone sialoprotein by osteoclastic tartrate-resistant acid phosphatase. Modulation of osteoclast adhesion in vitro, *The Journal of biological chemistry* 269, 14853-14856.
 23. Nemir, M., DeVouge, M. W., and Mukherjee, B. B. (1989) Normal rat kidney cells secrete both phosphorylated and nonphosphorylated forms of osteopontin showing different physiological properties, *The Journal of biological chemistry* 264, 18202-18208.
 24. Katayama, Y., House, C. M., Udagawa, N., Kazama, J. J., McFarland, R. J., Martin, T. J., and Findlay, D. M. (1998) Casein kinase 2 phosphorylation of recombinant rat osteopontin enhances adhesion of osteoclasts but not osteoblasts, *J Cell Physiol* 176, 179-187.
 25. Christensen, B., Klaning, E., Nielsen, M. S., Andersen, M. H., and Sorensen, E. S. (2012) C-terminal modification of osteopontin inhibits interaction with the alphaVbeta3-integrin, *The Journal of biological chemistry* 287, 3788-3797.
 26. Kato, K., Jeanneau, C., Tarp, M. A., Benet-Pages, A., Lorenz-Depiereux, B., Bennett, E. P., Mandel, U., Strom, T. M., and Clausen, H. (2006) Polypeptide GalNAc-transferase T3 and familial tumoral calcinosis. Secretion of fibroblast growth factor 23 requires O-glycosylation, *The Journal of biological chemistry* 281, 18370-18377.
 27. Schjoldager, K. T., Vester-Christensen, M. B., Bennett, E. P., Lavery, S. B., Schwientek, T., Yin, W., Blixt, O., and Clausen, H. (2010) O-glycosylation modulates proprotein convertase activation of angiopoietin-like protein 3: possible role of polypeptide GalNAc-transferase-2 in regulation of concentrations of plasma lipids, *The Journal of biological chemistry* 285, 36293-36303.
 28. Rolain, T., Bernard, E., Beaussart, A., Degand, H., Courtin, P., Egge-Jacobsen, W., Bron, P. A., Morsomme, P., Kleerebezem, M., Chapot-Chartier, M. P., Dufrene, Y. F., and Hols, P. (2013) O-glycosylation as a novel control mechanism of peptidoglycan

- hydrolase activity, *The Journal of biological chemistry* 288, 22233-22247.
29. Gerken, T. A., Butenhof, K. J., and Shogren, R. (1989) Effects of glycosylation on the conformation and dynamics of O-linked glycoproteins: carbon-13 NMR studies of ovine submaxillary mucin, *Biochemistry* 28, 5536-5543.
 30. Dwek, R. A. (1995) Glycobiology: "towards understanding the function of sugars", *Biochemical Society transactions* 23, 1-25.
 31. Julien, S., Lagadec, C., Krzewinski-Recchi, M. A., Courtand, G., Le Bourhis, X., and Delannoy, P. (2005) Stable expression of sialyl-Tn antigen in T47-D cells induces a decrease of cell adhesion and an increase of cell migration, *Breast Cancer Res Treat* 90, 77-84.
 32. Clement, M., Rocher, J., Loirand, G., and Le Pendu, J. (2004) Expression of sialyl-Tn epitopes on beta1 integrin alters epithelial cell phenotype, proliferation and haptotaxis, *Journal of cell science* 117, 5059-5069.
 33. Maxson, J. E., Luty, S. B., MacManiman, J. D., Abel, M. L., Druker, B. J., and Tyner, J. W. (2014) Ligand independence of the T618I mutation in the colony-stimulating factor 3 receptor (CSF3R) protein results from loss of O-linked glycosylation and increased receptor dimerization, *The Journal of biological chemistry* 289, 5820-5827.
 34. Goth, C. K., Halim, A., Khetarpal, S. A., Rader, D. J., Clausen, H., and Schjoldager, K. T. (2015) A systematic study of modulation of ADAM-mediated ectodomain shedding by site-specific O-glycosylation, *Proceedings of the National Academy of Sciences of the United States of America* 112, 14623-14628.
 35. Kariya, Y., and Gu, J. (2011) N-glycosylation of ss4 integrin controls the adhesion and motility of keratinocytes, *PloS one* 6, e27084.
 36. Christensen, B., Zachariae, E. D., Scavenius, C., Kloverpris, S., Oxvig, C., Petersen, S. V., Enghild, J. J., and Sorensen, E. S. (2016) Transglutaminase 2-Catalyzed Intramolecular Cross-Linking of Osteopontin, *Biochemistry* 55, 294-303.
 37. Segers-Nolten, I. M., Wilhelmus, M. M., Veldhuis, G., van Rooijen, B. D., Drukarch, B., and Subramaniam, V. (2008) Tissue transglutaminase modulates alpha-synuclein oligomerization, *Protein science : a publication of the Protein Society* 17, 1395-1402.
 38. Minai-Tehrani, A., Chang, S. H., Park, S. B., and Cho, M. H. (2013) The Oglycosylation mutant osteopontin alters lung cancer cell growth and migration in vitro and in vivo, *International journal of molecular medicine* 32, 1137-1149.
 39. Bennett, E. P., Mandel, U., Clausen, H., Gerken, T. A., Fritz, T. A., and Tabak, L. A.

- (2012) Control of mucin-type O-glycosylation: a classification of the polypeptide GalNAc-transferase gene family, *Glycobiology* 22, 736-756.
40. Muller, S., Alving, K., Peter-Katalinic, J., Zachara, N., Gooley, A. A., and Hanisch, F. G. (1999) High density O-glycosylation on tandem repeat peptide from secretory MUC1 of T47D breast cancer cells, *The Journal of biological chemistry* 274, 18165-18172.
 41. Muller, S., Goletz, S., Packer, N., Gooley, A., Lawson, A. M., and Hanisch, F. G. (1997) Localization of O-glycosylation sites on glycopeptide fragments from lactation-associated MUC1. All putative sites within the tandem repeat are glycosylation targets in vivo, *The Journal of biological chemistry* 272, 24780-24793.
 42. Seguchi, T., Merkle, R. K., Ono, M., Kuwano, M., and Cummings, R. D. (1991) The dysfunctional LDL receptor in a monensin-resistant mutant of Chinese hamster ovary cells lacks selected O-linked oligosaccharides, *Archives of biochemistry and biophysics* 284, 245-256.
 43. Yoshimura, A., Yoshida, T., Seguchi, T., Waki, M., Ono, M., and Kuwano, M. (1987) Low binding capacity and altered O-linked glycosylation of low density lipoprotein receptor in a monensin-resistant mutant of Chinese hamster ovary cells, *The Journal of biological chemistry* 262, 13299-13308.
 44. Tagashira, M., Iijima, H., Isogai, Y., Hori, M., Takamatsu, S., Fujibayashi, Y., Yoshizawa-Kumagaye, K., Isaka, S., Nakajima, K., Yamamoto, T., Teshima, T., and Toma, K. (2001) Site-dependent effect of O-glycosylation on the conformation and biological activity of calcitonin, *Biochemistry* 40, 11090-11095.
 45. Shanmugam, V., Chackalaparampil, I., Kundu, G. C., Mukherjee, A. B., and Mukherjee, B. B. (1997) Altered sialylation of osteopontin prevents its receptor-mediated binding on the surface of oncogenically transformed tsB77 cells, *Biochemistry* 36, 5729-5738.
 46. Gerken, T. A., Revoredo, L., Thome, J. J., Tabak, L. A., Vester-Christensen, M. B., Clausen, H., Gahlay, G. K., Jarvis, D. L., Johnson, R. W., Moniz, H. A., and Moremen, K. (2013) The lectin domain of the polypeptide GalNAc transferase family of glycosyltransferases (ppGalNAc Ts) acts as a switch directing glycopeptide substrate glycosylation in an N- or C-terminal direction, further controlling mucin type O-glycosylation, *The Journal of biological chemistry* 288, 19900-19914.
 47. Tagliabracci, V. S., Engel, J. L., Wiley, S. E., Xiao, J., Gonzalez, D. J., Nidumanda Appaiah, H., Koller, A., Nizet, V., White, K. E., and Dixon, J. E. (2014) Dynamic

regulation of FGF23 by Fam20C phosphorylation, GalNAc-T3 glycosylation, and furin proteolysis, *Proceedings of the National Academy of Sciences of the United States of America* 111, 5520-5525.

48. Pinho, S. S., and Reis, C. A. (2015) Glycosylation in cancer: mechanisms and clinical implications, *Nature reviews. Cancer* 15, 540-555.

Fig. 1

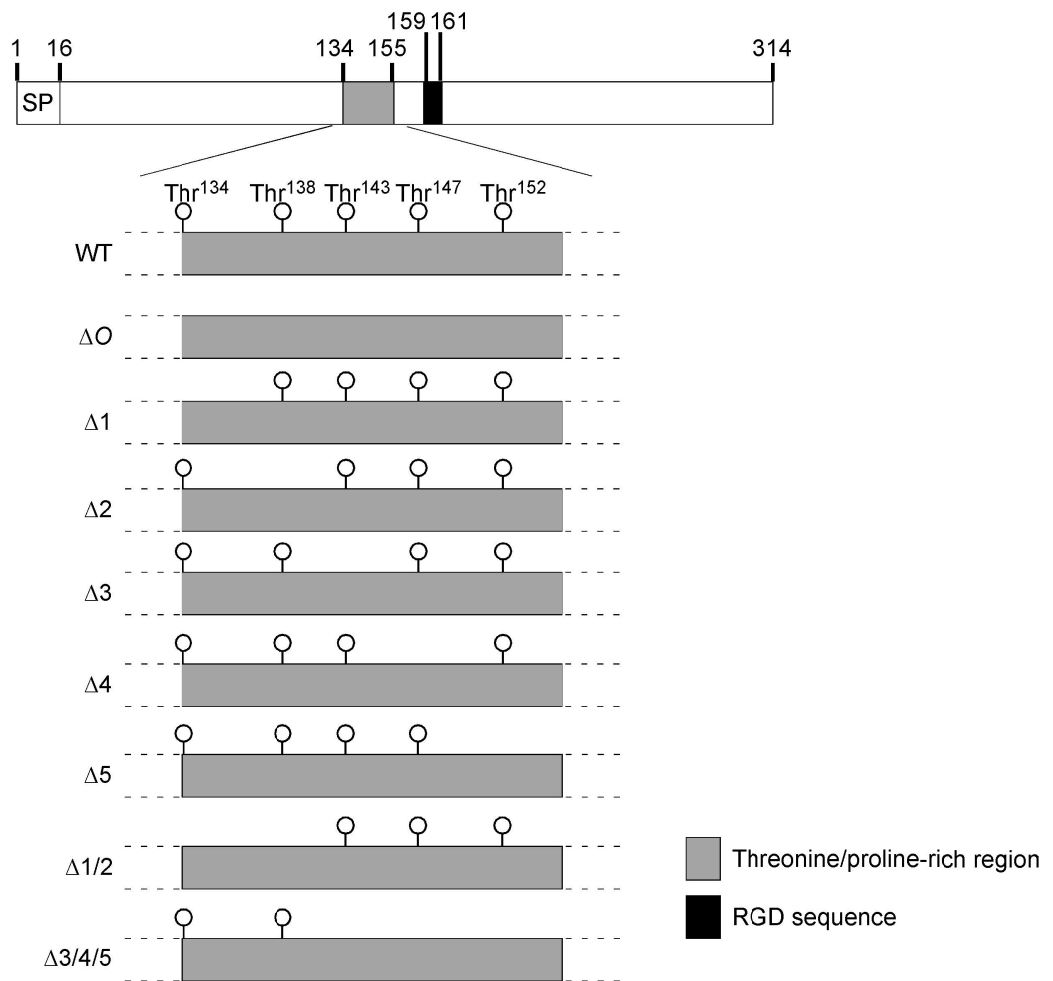


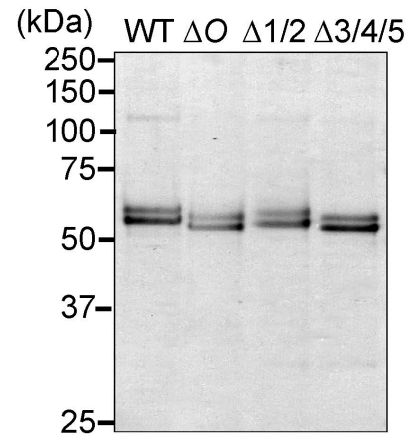
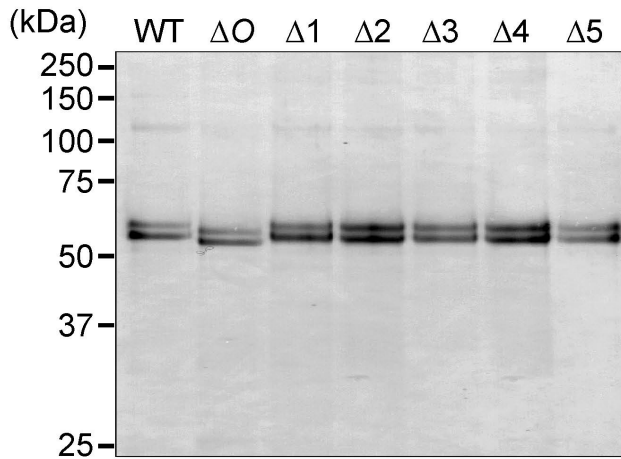
Figure 1. Schematic diagram of human WT-OPN and *O*-glycosylation site-defective OPN depicting *O*-glycosylation sites in threonine/proline-rich region.

O-glycosylation sites are shown by flags. Numbers indicate the number of amino acid residues.

SP: signal peptide.

Fig. 2

A



B

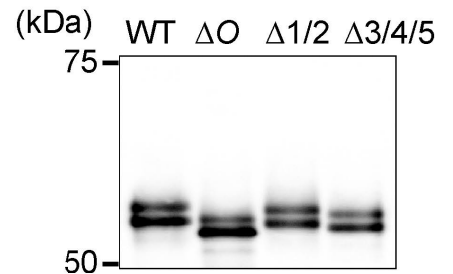
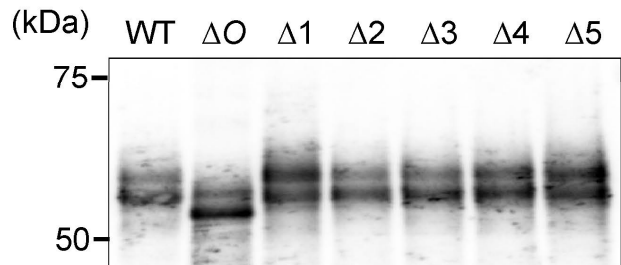


Figure 2. CBB staining and Western blot of purified WT-OPN and *O*-glycosylation site-defective OPN.

Purified rOPNs were run on 5–20% (A) or 7.5% (B) SDS/PAGE gel under reducing conditions, followed by CBB staining (A) or Western blot with an anti-OPN antibody (B). Data are representative of three independent experiments.

Fig. 3

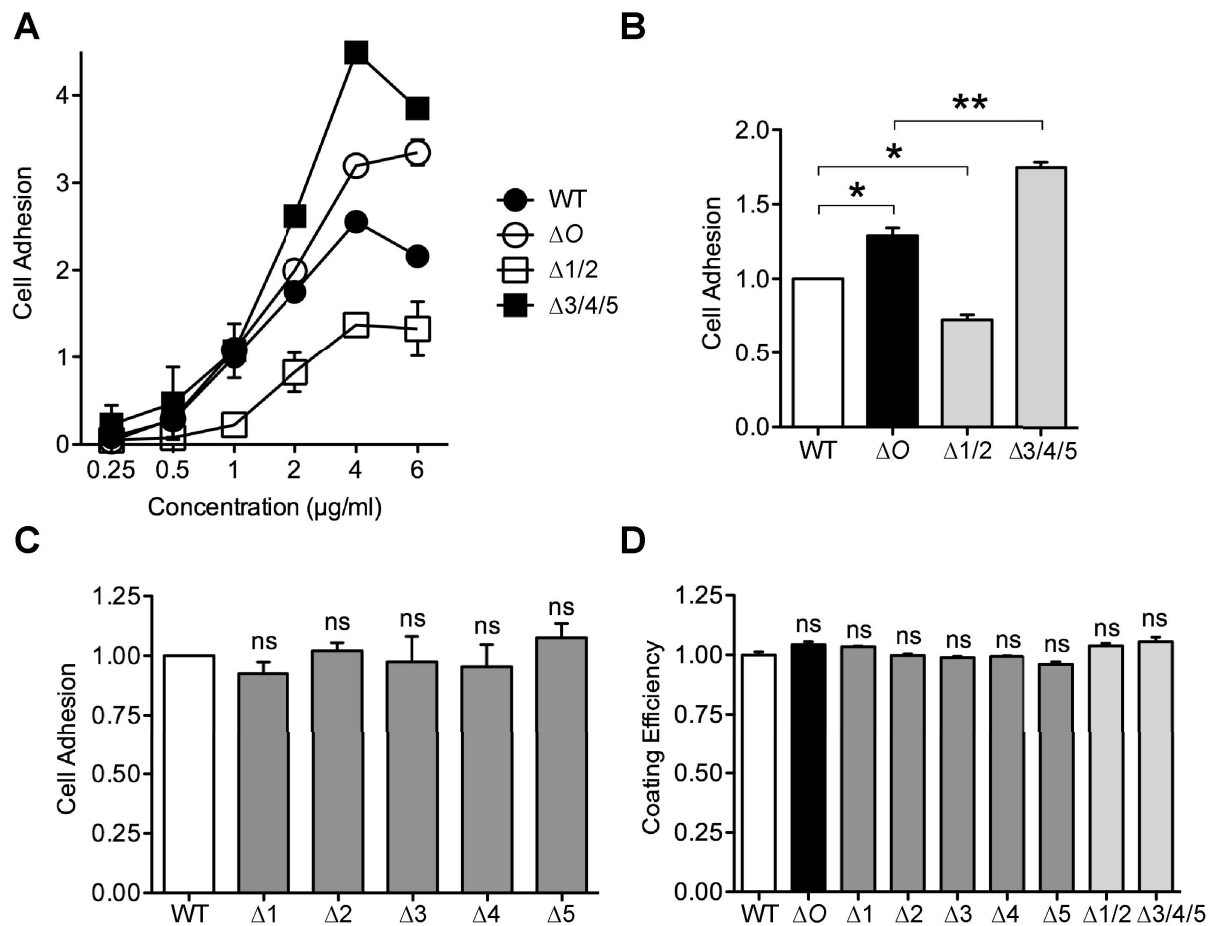


Figure 3. Effect of site-specific *O*-glycosylation on cell adhesion activity of OPN.

(A and B) Cell adhesion activity of the WT and multiple *O*-glycosylation site-deficient OPN against HT1080 cells (A) and MDA-MB231 cells (B). (C) Cell adhesion activity of the WT and single *O*-glycosylation site-deficient OPN against MDA-MB231 cells. In B and C, each well of a 96-well plate was coated with 50 μl of 2 $\mu\text{g/ml}$ rOPNs for the assays. The relative number of adherent cells on WT-OPN was taken as 1.0. (D) Coating efficiency of rOPNs for the wells of a 96-well plate (50 μl of 2 $\mu\text{g/ml}$) was determined by ELISA using an anti-OPN antibody. Results are mean \pm SEM for two or three independent experiments, each conducted in triplicate. ns, not significant. * $P < 0.05$. ** $P < 0.01$.

Fig. 4

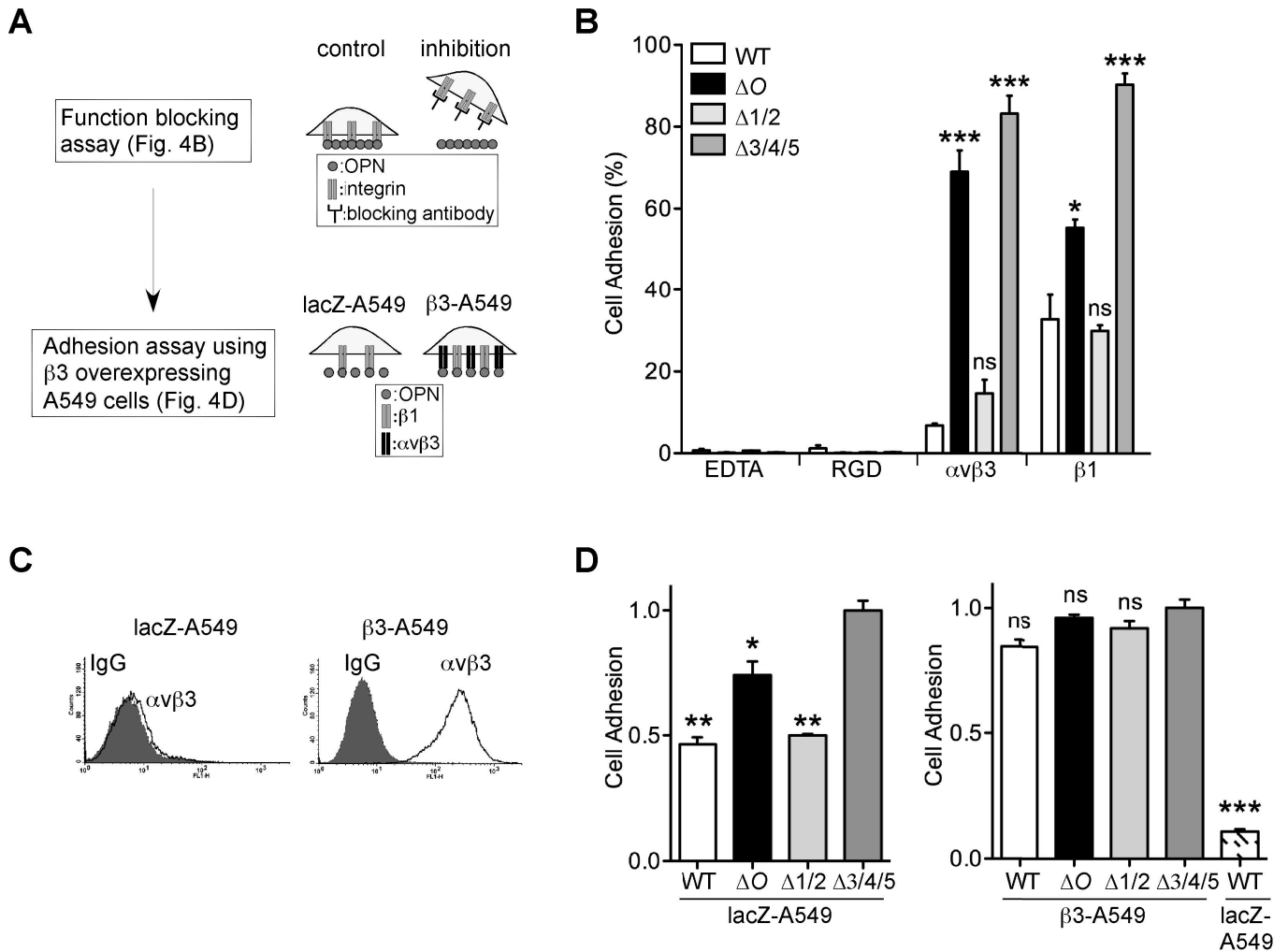


Figure 4. Effect of site-specific *O*-glycosylation on associations of OPN with integrins.

(A) Diagram outlining the experiments in Figure 4. (B) Inhibitory effects of EDTA, RGD peptide, and function-blocking antibodies against $\alpha v\beta 3$ and $\beta 1$ integrins on cell adhesion activity of rOPNs. MDA-MB231 cells in serum-free media pre-treated with PBS, 5 mM EDTA, GRGESP (RGE) and GRGDSP (RGD) peptides (100 μ M), or control mouse IgG, anti- $\alpha v\beta 3$ integrin antibody (LM609, 5 μ g/ml), and anti- $\beta 1$ integrin antibody (JB1A, 1:8000) were plated into the wells that were coated with 8 μ g/ml rOPN. After incubation for 1 h, non-adherent cells were removed and adherent cells were fixed and stained with crystal violet. Results of inhibitory assays are shown as the relative number of adherent cells in the presence of EDTA, RGD peptide, or the integrin antibodies, which was 100% for respective controls, PBS, RGE peptide, or mouse IgG. Results are mean \pm SEM for three independent experiments, each conducted in

triplicate. ns, not significant vs. WT. * $P < 0.05$ vs. WT. 1 *** $P < 0.001$ vs. WT. (C) FACS analysis of cell surface expression levels of $\alpha v\beta 3$ integrin on A549 cells overexpressing lacZ (lacZ-A549) and $\beta 3$ integrin ($\beta 3$ -A549). (D) Cell adhesion activity of rOPNs against lacZ-A549 (left panel) and $\beta 3$ -A549 (right panel) cells. Each transfectant in the serum-free medium was plated into rOPN (50 μ l of 10 μ g/ml for lacZ-A549 and 0.1 μ g/ml for $\beta 3$ -A549)-coated wells. The relative number of adherent cells on $\Delta 3/4/5$ was taken as 1.0. Results are mean \pm SEM for two or three independent experiments, each conducted in triplicate. ns, not significant. * $P < 0.05$. ** $P < 0.01$. *** $P < 0.001$.

Fig. 5

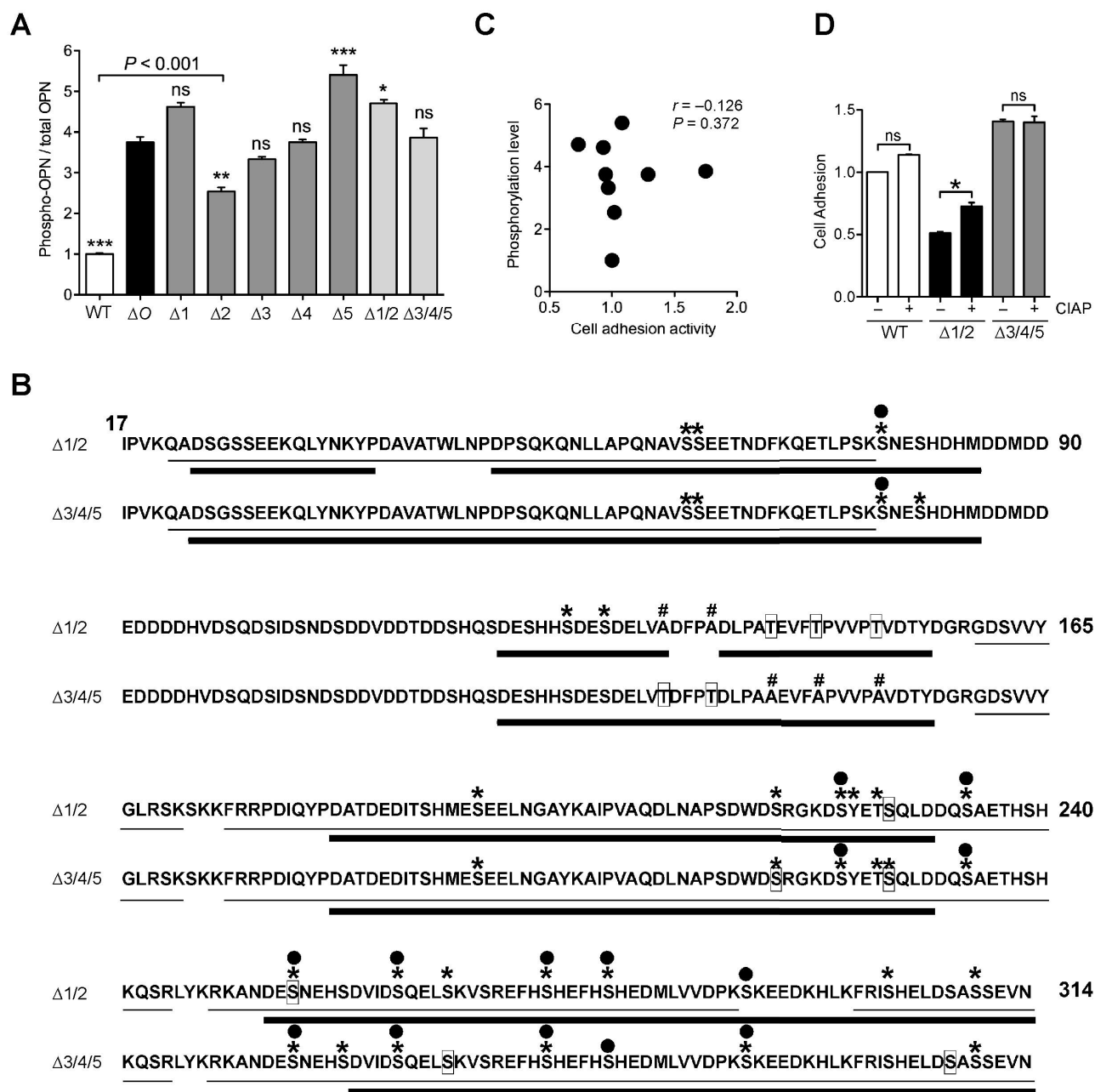


Figure 5. Deletion of site-specific *O*-glycan induced distinct phosphorylation states in OPN.

(A) Quantitative analysis of the phosphorylation level of rOPNs (50 μ l of 0.5 μ g/ml) by ELISA. Each bar represents the ratio of phosphorylated OPN to total OPN. Results are mean \pm SEM for two independent experiments, each conducted in triplicate. * P < 0.05 vs. ΔO , ** P < 0.01 vs.

ΔO , *** $P < 0.001$ vs. ΔO . ns, not significant vs. ΔO . (B) *O*-glycosylation and phosphorylation of $\Delta 1/2$ and $\Delta 3/4/5$ identified by LC-MS/MS analysis. Phosphorylated sites are marked with asterisks (*), and *O*-glycosylated residues are in boxes. The residues covered by this mass analysis are underlined. Thin underline: mixture of trypsin and lysyl endopeptidase treatment. Thick underline: Asp-N treatment. Mutated residues (Thr to Ala) are marked with number signs (#). Black circles indicate the identified phosphorylated sites in the WT in our previous study (Kariya Y., et al., 2014 Biochem. J. p93-102). (C) Correlation analysis between phosphorylation level and cell adhesion activity in OPN. The phosphorylation level was not correlated with cell adhesion activity in OPN ($r = -0.126$, $P = 0.372$). The values used in this figure were derived from the data in Figure 3 and Figure 5. (D) Effect of de-phosphorylation on cell adhesion activity of rOPN. MDA-MB231 cells were plated into the wells that were coated with 4 $\mu\text{g/ml}$ rOPN pre-treated with or without phosphatase, CIAP. Adherent cells were fixed and stained with crystal violet. The average number of adherent cells to the WT without the CIAP treatment was set at 1.0. Results are mean \pm SEM for two independent experiments, each conducted in triplicate. ns, not significant. * $P < 0.05$.

Table S1 The list of identified peptides from trypsin-digested Δ 1/2-OPN

Sequence	Modifications	Charge	MH+[Da]	Δ M [ppm]	RT [min]
AIPVAQDLNAPSDWDSR		2	1854.90215	2.15	58.74
AIPVAQDLNAPSDWDSRGK		3	2040.01480	0.10	53.23
AIPVAQDLNAPSDWDSRGKDSYETSQLDDQSAETHSHK		5	4198.92347	1.16	51.36
ANDESNEHSDVIDSQELSK	Ser ²⁵⁴ [Hex(1)HexNAc(1)]	3	2482.06089	0.84	35.04
ANDESNEHSDVIDSQELSK		2	2116.92436	-1.06	36.68
ANDESNEHSDVIDSQELSK	Ser ²⁵⁴ (Phospho)	2	2196.89238	-0.26	39.56
ANDESNEHSDVIDSQELSK	Ser ²⁶³ (Phospho)	2	2196.89409	0.52	38.33
ANDESNEHSDVIDSQELSKVSR		3	2459.13205	1.57	38.06
DSYETSQLDDQSAETHSHK	Ser ²³⁴ (Phospho)	3	2257.89219	1.78	31.81
DSYETSQLDDQSAETHSHK		2	2177.92314	0.60	30.28
DSYETSQLDDQSAETHSHKQSR	Ser ²³⁴ (Phospho)	4	2629.07924	-0.25	28.98
DSYETSQLDDQSAETHSHKQSR		3	2549.10257	-4.31	27.53
EFHSHEFHSHEDMLVDPK		4	2320.04873	1.51	41.65
FRISHELDSASSEVNHHHHHHH		3	2513.15787	0.49	32.59
FRRPDIQYPDATDEDITSHMESEELNGAYK		4	3543.59829	0.36	51.68
GDSVYGLR		2	965.50481	-0.31	31.92
GDSVYGLRSK		3	1180.63199	-0.10	32.93
GKDSYETSQLDDQSAETHSHK	Tyr ²²⁵ (Phospho)	4	2443.00771	1.27	28.98
GKDSYETSQLDDQSAETHSHK	Ser ²²⁸ [Hex(1)HexNAc(1)]	4	2728.17373	1.19	25.78
GKDSYETSQLDDQSAETHSHK		2	2363.04302	2.01	27.08
GKDSYETSQLDDQSAETHSHK	Ser ²³⁴ (Phospho)	2	2522.97612	2.06	30.39
GKDSYETSQLDDQSAETHSHKQSR		3	2734.23008	0.03	24.79
GKDSYETSQLDDQSAETHSHKQSR	Ser ²³⁴ (Phospho)	3	2814.19590	-0.16	25.62
ISHELDSASSEVNHHHHHHH	Ser ³⁰³ (Phospho)	4	2289.95058	-1.24	24.31
ISHELDSASSEVNHHHHHHH	Ser ³¹⁰ (Phospho)	4	2289.95449	0.47	21.69
ISHELDSASSEVNHHHHHHH		2	2209.99248	2.44	21.80
KANDESNEHSDVIDSQELSK	Ser ²⁶³ (Phospho)	3	2324.99137	1.49	34.25
KANDESNEHSDVIDSQELSK	Ser ²⁵⁴ (Phospho); Ser ²⁶³ (Phospho)	3	2404.95243	-0.76	36.64
KANDESNEHSDVIDSQELSK	Ser ²⁶⁷ (Phospho)	3	2528.06577	-0.60	33.75
KANDESNEHSDVIDSQELSK		2	2245.02349	0.85	33.06
KANDESNEHSDVIDSQELSK	Ser ²⁵⁴ (Phospho)	2	2324.98931	0.60	35.13
QADSGSSEEKQLYNK		2	1683.78581	2.21	26.30
QADSGSSEEKQLYNKYPDAVATWLNPDPSQK		4	3466.63881	-0.30	62.73
QETLPSK		2	802.43132	0.97	22.17
QLYNKYPDAVATWLNPDPSQK		3	2448.21384	-2.30	61.47
QNLLAPQNAVSEETNDFK		2	2105.01470	0.03	63.13
QNLLAPQNAVSEETNDFK	Ser ⁶² (Phospho)	2	2184.98076	-0.10	56.39
QNLLAPQNAVSEETNDFK	Ser ⁶³ (Phospho)	2	2184.98100	0.01	57.40
QNLLAPQNAVSEETNDFKQETLPSK		3	2888.44077	4.65	54.90
QNLLAPQNAVSEETNDFKQETLPSK	Ser ⁶³ (Phospho)	3	2968.39469	0.34	58.27

QNLLAPQNAV S SEETNDFKQETLPSK	Ser⁶²(Phospho)	3	2968.39652	0.96	57.18
RKANDESNEHSDVID S QELSK	Ser²⁶³(Phospho)	3	2481.08933	0.12	31.21
RKANDE S NEHSDVIDSQELSK	Ser²⁵⁴(Phospho)	3	2481.09098	0.78	31.72
RKANDE S NEHSDVID S QELSK	Ser²⁵⁴(Phospho); Ser²⁶³(Phospho)	3	2561.05606	0.27	33.54
RKANDESNEHSDVIDSQELSK		2	2401.12236	-0.14	29.85
RPDIQYPDATDEDITSHMESEELNGAYK		4	3224.43740	1.50	56.83
RPDIQYPDATDEDITSHME S EELNGAYK	Ser¹⁹⁵(Phospho)	3	3400.34946	-3.14	54.25
VSREFHSHEFHSHEDMLLVDPK		4	2678.24306	0.50	34.92
YPDAVATWLNPDPSQK		2	1801.87627	0.36	63.81

Table S2 The list of identified peptides from Asp-N-digested Δ 1/2-OPN

Sequence	Modifications	Charge	MH+[Da]	Δ M [ppm]	RT [min]
DATDEDITSHMESEELNGAYKAIPVAQ		3	2950.32804	0.70	57.98
DEDITSHMESEELNGAYKAIPVAQ	Ser ¹⁹⁵ (Phospho)	3	2743.18265	0.76	60.53
DEDITSHMESEELNGAYKAIPVAQDLNAPS		3	3260.47483	-4.69	53.21
DESDELVA		2	877.37871	0.15	40.50
DESHHSDDELVA		2	1569.63005	0.03	30.60
DESHHSDDELVA	Ser ¹²⁹ (Phospho)	2	1649.59831	1.20	35.71
DESHHSDDELVA	Ser ¹²⁶ (Phospho)	2	1649.59758	0.75	35.20
DESNEHSDVI		2	1144.47624	0.80	30.46
DFKQETLPSKSNESH	Ser ⁷⁸ (Phospho)	2	1826.79607	0.19	33.02
DFKQETLPSKSNESH		2	1746.82891	-0.27	28.60
DFKQETLPSKSNESHDM		4	2145.95302	1.10	27.91
DKHLKFRISHEL		2	1522.85124	1.52	37.21
DLNAPSDW		2	917.40019	0.23	55.56
DLNAPSDWDSRGK		2	1460.67766	0.78	39.09
DLNAPSDWDSRGK	Ser ²¹⁹ (Phospho)	2	1540.64726	2.86	40.82
DLPATEVFTPVVPTV		2	1584.85234	0.20	82.17
DMLVDPKSKEE		2	1389.69341	0.23	39.06
DMLVDPKSKEEDKHLKFRISHEL		3	2909.52005	0.33	45.74
DPSQKQNLAPQNAVSSSEETN		2	2270.09014	0.24	46.73
DSASSEVNHSHHHH		3	1630.68619	0.48	15.60
DSGSSEKQLYNKYP		2	1744.80388	0.80	39.79
DSQELSKVSREFHSHEFSHE		3	2552.15732	0.92	42.47
DSQELSKVSREFHSHEFSHE	Ser ²⁸⁰ (Phospho)	4	2632.12295	0.62	43.57
DSRGKDSYETSQ		2	1485.68303	0.94	31.72
DSRGKDSYETSQ	Ser ²²⁴ (Phospho)	2	1565.65093	1.89	34.18
DSRGKDSYETSQ	Thr ²²⁷ (Phospho)	2	1565.64263	-3.41	34.69
DSRGKDSYETSQ	Ser ²¹⁹ (Phospho)	2	1565.65300	3.21	35.55
DSRGKDSYETSQ		2	1600.71062	1.27	29.57
DSYETSQ		2	1057.43205	0.00	37.74
DVIDSQELSKVSREFHSHEFSHE		3	2879.33951	1.77	54.88
DVIDSQELSKVSREFHSHEFSHE	Ser ²⁷⁵ (Phospho)	4	2959.30361	0.97	55.78

Table S3 The list of identified peptides from trypsin-digested $\Delta 3/4/5$ -OPN

Sequence	Modifications	Charge	MH+[Da]	ΔM [ppm]	RT [min]
AIPVAQDLNAPSDWDSR		2	1854.89714	-0.55	58.97
AIPVAQDLNAPSDWDSRGK		3	2040.01682	1.09	53.61
AIPVAQDLNAPSDWDSRGKDSYETSQLDDQSAETHSHK		4	4198.91811	-0.11	51.44
ANDESNEHSDVIDSQELSK	Ser ²⁵⁴ (Phospho)	2	2196.89141	-0.70	39.82
ANDESNEHSDVIDSQELSK		2	2116.92851	0.90	36.09
ANDESNEHSDVIDSQELSK	Ser ²⁶³ (Phospho)	2	2196.89409	0.52	38.18
ANDESNEHSDVIDSQELSK	Ser ²⁵⁸ (Phospho)	3	2196.89499	0.93	39.13
ANDESNEHSDVIDSQELSKVSR		3	2459.13572	3.06	37.91
ANDESNEHSDVIDSQELSKVSR	Ser ²⁶³ (Phospho)	4	2539.09145	-1.21	43.87
DSYETSQLDDQSAETHSHK	Ser ²³⁴ (Phospho)	2	2257.88872	0.25	31.65
DSYETSQLDDQSAETHSHK		2	2177.92314	0.60	30.31
DSYETSQLDDQSAETHSHKQSR	Ser ²³⁴ (Phospho)	3	2629.08084	0.36	29.23
DSYETSQLDDQSAETHSHKQSR		3	2549.11521	0.65	28.09
EFHSHEFHSHEDMLVDPK		4	2320.04751	0.98	41.75
FRISHELDSASSEVNHHHHHHH		4	2513.15932	1.07	32.69
FRRPDIQYPDATDEDITSHMESEELNGAYK		5	3543.58962	-2.09	52.13
GDSVYGLR		2	965.50633	1.27	40.85
GDSVYGLRSK		3	1180.63391	1.53	32.83
GKDSYETSQLDDQSAETHSHK	Ser ²²⁴ (Phospho); Ser ²³⁴ (Phospho)	3	2522.96994	-0.39	30.89
GKDSYETSQLDDQSAETHSHK		3	2363.03922	0.40	25.72
GKDSYETSQLDDQSAETHSHK	Ser ²²⁸ (Phospho)	4	2808.12739	-3.35	28.33
GKDSYETSQLDDQSAETHSHK	Thr ²²⁷ (Phospho)	4	2443.00454	-0.03	29.65
GKDSYETSQLDDQSAETHSHK	Ser ²³⁴ (Phospho)	3	2443.00760	1.23	28.36
GKDSYETSQLDDQSAETHSHK	Ser ²²⁸ [Hex(1)HexNAc(1)]	4	2728.17104	0.21	25.82
GKDSYETSQLDDQSAETHSHKQSR	Ser ²²⁴ (Phospho); Ser ²³⁴ (Phospho)	3	2894.16446	0.62	28.05
GKDSYETSQLDDQSAETHSHKQSR		2	2734.23442	1.62	24.78
GKDSYETSQLDDQSAETHSHKQSR	Ser ²³⁴ (Phospho)	4	2814.20717	3.85	26.37
GKDSYETSQLDDQSAETHSHKQSR	Ser ²²⁴ (Phospho)	4	2814.19741	0.38	26.92
HLKFR		2	700.42583	0.71	19.81
ISHELDSASSEVNHHHHHHH	Ser ³¹⁰ (Phospho)	2	2289.96099	3.30	21.29
ISHELDSASSEVNHHHHHHH		2	2209.99126	1.89	21.99
ISHELDSASSEVNHHHHHHH	Ser ³⁰⁸ (HexNAc)	5	2413.08012	5.66	21.10
ISHELDSASSEVNHHHHHHH	Ser ³⁰⁸ [Hex(1)HexNAc(1)]	5	2575.11121	-3.14	20.77
KANDESNEHSDVIDSQELSK	Ser ²⁵⁴ (Phospho); Ser ²⁶³ (Phospho)	4	2404.95815	1.62	36.80
KANDESNEHSDVIDSQELSK		2	2245.02202	0.20	31.28
KANDESNEHSDVIDSQELSK	Ser ²⁵⁴ (Phospho)	3	2324.99649	3.69	35.22
KANDESNEHSDVIDSQELSK	Ser ²⁶⁷ (HexNAc)	3	2528.07035	1.21	34.94
KANDESNEHSDVIDSQELSK	Ser ²⁶³ (Phospho)	4	2324.99257	2.01	34.06
KANDESNEHSDVIDSQELSK	Ser ²⁵⁸ (Phospho)	3	2324.98844	0.23	34.70
KANDESNEHSDVIDSQELSKVSR	Ser ²⁶³ (Phospho)	3	2667.19425	1.79	40.38

KANDESNEHSDVIDSQELSKVSR		3	2587.22733	1.61	37.90
QADSGSSEEKQLYNK		2	1683.78777	3.37	26.32
QADSGSSEEKQLYNKYDAVATWLNPDPSQK		4	3466.64345	1.04	62.64
QETLPSK		2	802.43144	1.13	22.21
QLYNKYDAVATWLNPDPSQK		3	2448.21787	-0.66	64.57
QNLLAPQNAVSSEETNDFK		2	2105.01543	0.37	63.19
QNLLAPQNAVSEETNDFK	Ser⁶²(Phospho)	2	2184.98076	-0.10	56.53
QNLLAPQNAVSEETNDFKQETLPSK	Ser⁶³(Phospho)	3	2968.39634	0.90	58.22
QNLLAPQNAVSSEETNDFKQETLPSK		3	2888.42740	0.02	54.41
RKANDESNEHSDVIDSQELSK	Ser²⁵⁴(Phospho); Ser²⁶³(Phospho)	3	2561.05680	0.56	33.48
RKANDESNEHSDVIDSQELSK	Ser²⁵⁴(Phospho)	3	2481.09720	3.29	31.61
RKANDESNEHSDVIDSQELSK		3	2401.11838	-1.80	30.80
RPDIQYPDATDEDITSHMSEELNGAYK	Ser¹⁹⁵(Phospho)	3	3320.39170	-0.64	52.40
RPDIQYPDATDEDITSHMESEELNGAYK		4	3224.43813	1.72	56.78
SKEEDKHLK		3	1113.58985	-0.06	7.50
VSREFHSHEFHSHEDMLLVDPK		4	2678.24306	0.50	35.35
VSREFHSHEFHSHEDMLLVDPK	Ser²⁷⁵(Phospho)	4	2758.21303	1.81	38.18
YDAVATWLNPDPSQK		2	1801.87688	0.70	64.17

Table S4 The list of identified peptides from Asp-N-digested Δ 3/4/5-OPN

Sequence	Modifications	Charge	MH+[Da]	Δ M [ppm]	RT [min]
DATDEDITSHMESEELNGAYKAIPVAQ		3	2950.32877	0.94	57.93
DAVATWLNLP		2	986.49407	-0.16	66.24
DEDITSHMESEELNGAYKAIPVAQ		3	2663.21756	1.25	55.93
DEDITSHMESEELNGAYKAIPVAQ	Ser ¹⁹⁵ (Phospho)	3	2743.18357	1.09	60.52
DELVTDFPT		2	1036.48442	1.00	61.14
DESHHSDESDELVT		2	1599.64202	0.90	29.66
DFKQETLPSKSNESH		2	1746.83403	2.66	29.03
DFKQETLPSKSNESH	Ser ⁷⁸ (Phospho)	2	1826.79680	0.60	32.87
DFKQETLPSKSNESH	Ser ⁸¹ (Phospho)	3	1826.79691	0.66	32.31
DFKQETLPSKSNESHDM		3	2145.95359	1.37	27.78
DITSHMESEELNGAYKAIPVAQ		3	2419.14695	0.93	55.02
DKHLKFRISHL		2	1522.84783	-0.73	37.43
DLNAPSDW		2	917.40032	0.37	55.29
DLNAPSDWDSRGK		2	1460.67790	0.95	38.79
DLNAPSDWDSRGK	Ser ²¹⁹ (Phospho)	2	1540.64678	2.55	40.94
DLNAPSDWDSRGK	Ser ²¹⁹ [Hex(1)HexNAc(1)]	3	1825.80027	-4.63	45.63
DLPAAEVFAPVPAVDY		2	1873.95915	0.46	87.43
DMLVDPKSKEE		2	1389.69353	0.31	39.41
DMLVDPKSKEE	Ser ²⁹¹ (Phospho)	2	1469.66081	0.95	42.79
DMLVDPKSKEEDKHLKFRISHL		4	2909.52236	1.12	48.07
DPSQKQNLLAPQNAVSSEETN		2	2270.09087	0.56	46.61
DSASSEVNHSHHHH		3	1630.68583	0.25	39.95
DSGSSEKQLYNKYP		2	1744.80388	0.80	39.61
DSQELSKVSREFHSHEFSHE		4	2552.16152	2.56	42.14
DSRGKDSYETSQL	Ser ²²⁴ (Phospho)	2	1565.65056	1.65	34.00
DSRGKDSYETSQL		2	1485.68266	0.69	32.08
DSRGKDSYETSQL	Ser ²¹⁹ (Phospho)	2	1565.65227	2.74	35.29
DSRGKDSYETSQLD		2	1600.71367	3.17	29.39
DSYETSQLD		2	1057.43230	0.23	37.04
DVIDSQELSKVSREFHSHEFSHE		4	2879.34145	2.44	55.17

Table S5 The list of glycosylated peptides in threonine/proline rich region of OPN identified by LC-MS/MS

Sequence	Modifications	Charge	MH+[Da]	ΔM [ppm]	RT [min]	Treated enzymes	Samples
VFT P VVPTVDTYDGR	T¹⁴⁷(HexNAc)	2	1868.92815	0.24	25.94	CIAP, V8, trypsin/LysC	$\Delta 1/2$ -OPN
VFT P VV P TVDTYDGR	T¹⁴⁷[Hex(1)HexNAc(1) or HexNAc]; T¹⁵² [HexNAc or Hex(1)HexNAc(1)]	3	2234.06449	2.05	24.89	CIAP, V8, trypsin/LysC	
VFT P VVPTVDTYDGR	T¹⁴⁷[Hex(1)HexNAc(1)]	3	2030.98624	2.81	25.20	CIAP, V8, trypsin/LysC	
VFT P VVPTV	T¹⁴⁷(HexNAc)	2	1161.64153	1.13	28.67	CIAP, V8, AspN	
DL P AT E VFT P VVPTVDTYDGRG	T¹⁴³(HexNAc); T¹⁴⁷(HexNAc)	3	2958.39511	-1.35	29.55	CIAP, AspN	
L V T D FP T DL P AA E	T¹³⁴(HexNAc)	2	1591.77580	1.24	29.23	CIAP, V8	$\Delta 3/4/5$ -OPN
S D EL V T D FP T DL P AA E	T¹³⁴[Hex(1)HexNAc(1)NeuAc(2)]	3	2667.12192	1.07	33.79	CIAP, V8, trypsin/LysC	
DEL V T D FP T DL P AA E	T¹³⁴(HexNAc)	2	1835.84477	0.76	31.00	CIAP, V8, AspN	
DEL V T D FP T DL P AA E	T¹³⁴(HexNAc); T¹³⁸(HexNAc)	2	2038.92522	1.21	29.98	CIAP, V8, AspN	
DEL V T D FP T	T¹³⁸[Hex(1)HexNAc(1)]	2	1401.61504	-0.38	24.39	CIAP, sialidase, AspN	
DEL V T D FP T	T¹³⁴(HexNAc)	2	1239.56352	0.62	25.76	CIAP, AspN	
DEL V T D FP T DL P AA E V F AP V PA V DT Y	T¹³⁴(HexNAc); T¹³⁸(HexNAc)	3	3297.58738	1.45	44.01	CIAP, AspN	

CIAP, calf intestine alkaline phosphatase; LysC, lysyl endopeptidase; AspN, endoproteinase Asp-N.

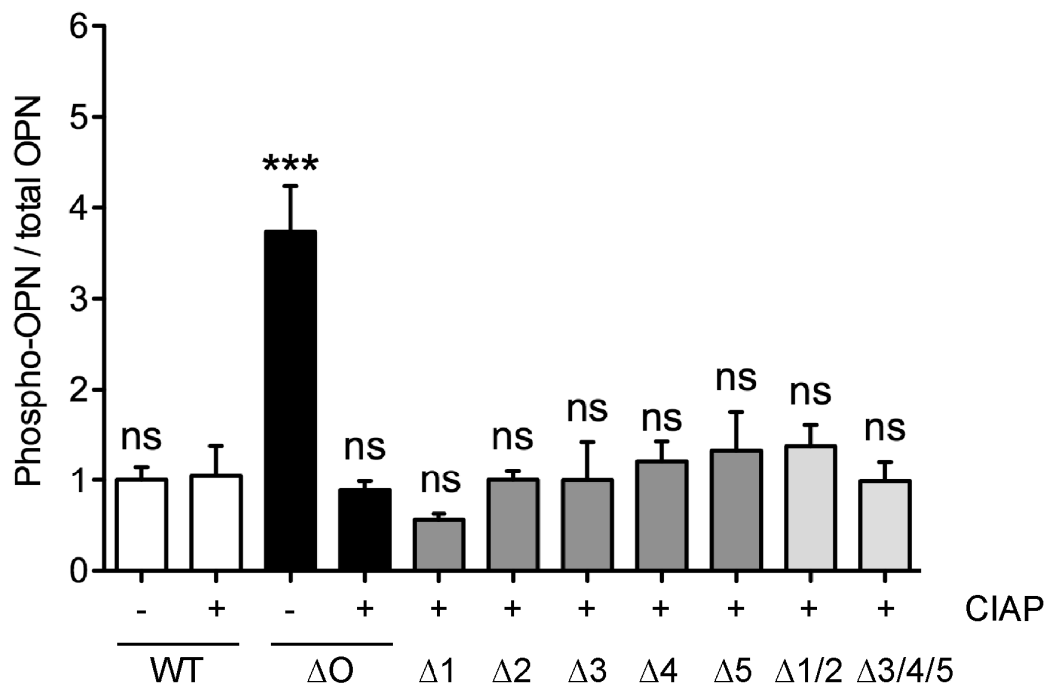


Fig. S1. Quantitative analysis of the phosphorylation level of rOPNs (50 μ l of 0.1 μ g/ml) pre-treated with (+) or without (-) phosphatase, CIAP by ELISA. Each bar represents the ratio of phosphorylated OPN to total OPN. The average ratio of phosphorylated WT-OPN to total WT-OPN without the CIAP treatment was set at 1.0. Results are mean \pm SEM for two independent experiments, each conducted in triplicate. *** $P < 0.001$ vs. WT with CIAP treatment. ns, not significant vs. WT with CIAP treatment.